The Arctic Ocean Spices Up

MARY-LOUISE TIMMERMANS

Yale University, New Haven, Connecticut

STEVEN R. JAYNE

Woods Hole Oceanographic Institution, Woods Hole, Massachusetts

(Manuscript received 25 January 2016, in final form 18 February 2016)

ABSTRACT

The contemporary Arctic Ocean differs markedly from midlatitude, ice-free, and relatively warm oceans in the context of density-compensating temperature and salinity variations. These variations are invaluable tracers in the midlatitudes, revealing essential fundamental physical processes of the oceans, on scales from millimeters to thousands of kilometers. However, in the cold Arctic Ocean, temperature variations have little effect on density, and a measure of density-compensating variations in temperature and salinity (i.e., spiciness) is not appropriate. In general, temperature is simply a passive tracer, which implies that most of the heat transported in the Arctic Ocean relies entirely on the ocean dynamics determined by the salinity field. It is shown, however, that as the Arctic Ocean warms up, temperature will take on a new role in setting dynamical balances. Under continued warming, there exists the possibility for a regime shift in the mechanisms by which heat is transported in the Arctic Ocean. This may result in a cap on the storage of deep-ocean heat, having profound implications for future predictions of Arctic sea ice.

1. Introduction

Temperature and salinity distributions in the Arctic Ocean are established by the seasonal cycle of solar forcing, which drives surface ocean warming and cooling and sea ice melt and growth cycles, precipitation, river influxes, and inflows from the Atlantic and Pacific Oceans. Mechanical redistribution and mixing by the winds, tidal mixing, and convective processes further modify temperature–salinity structure. Processes that govern the temperature–salinity properties are essential to the transport of ocean heat in the Arctic, which impacts the fate of sea ice (e.g., Maykut and Untersteiner 1971; Wettlaufer 1991; Perovich et al. 2008; Timmermans 2015) and has feedbacks to a warming atmosphere (e.g., Aagaard and Greisman 1975; Steele et al. 2008; Francis et al. 2009). This paper addresses the implications of a warming Arctic Ocean for its fundamental dynamics as they relate to the relative influences of temperature and salinity on density. In section 2, we review the concept of spiciness and describe its meaning in the context of the cold Arctic Ocean. In section 3, we compare and contrast the water column temperature–salinity structure of the Arctic Ocean and temperate Pacific Ocean. We show Arctic observations that reveal the potential for a change in the relative influences of temperature and salinity on density as the Arctic Ocean warms and describe the consequences of this for the structure and ventilation of the Arctic halocline.

2. Spiciness

Changes in seawater temperature and salinity may be scaled by the coefficients of thermal expansion α and haline contraction β,

$$\alpha = -\frac{1}{\rho}\frac{\partial\rho}{\partial\Theta}\bigg|_{S_A,p} \qquad \beta = \frac{1}{\rho}\frac{\partial\rho}{\partial S_A}\bigg|_{\Theta,p},$$

to express the total differential in density ρ as

$$\frac{d\rho}{\rho} = -\alpha d\Theta + \beta dS_A,$$

where S_A is Absolute Salinity, Θ is Conservative Temperature, and p is pressure; all computations here use

Corresponding author address: Mary-Louise Timmermans, Department of Geology and Geophysics, Yale University, 210 Whitney Ave., New Haven, CT 06511.
E-mail: mary-louise.timmermans@yale.edu

DOI: 10.1175/JPO-D-16-0027.1

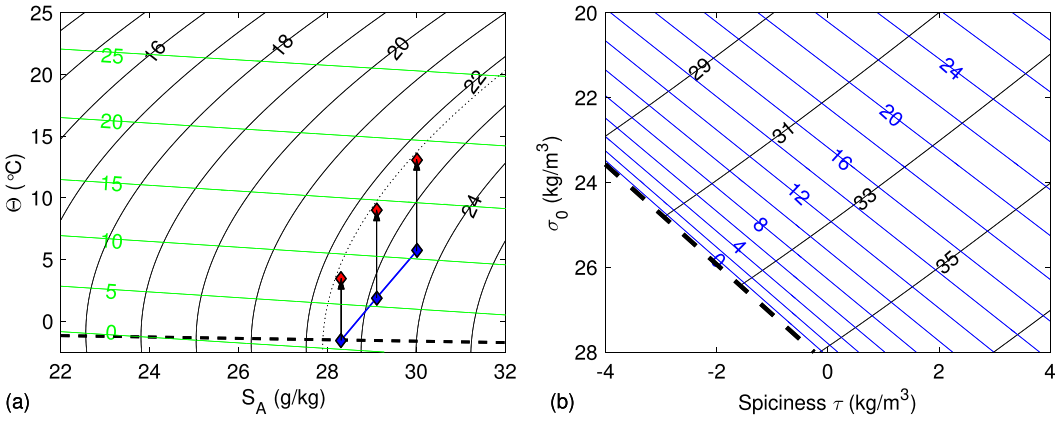

FIG. 1. (a) Conservative Temperature Θ (°C)–Absolute Salinity S_A (g kg^{-1}) plane with isolines of potential density at zero pressure σ_0 (black lines; kg m^{-3}) and coefficient of thermal expansion α (green lines; 10^{-5} °C^{-1}). The dashed black line indicates the freezing temperature at zero pressure. The blue diamonds indicate an example lateral surface ocean density gradient from the Chukchi Sea (rightmost diamonds) to the Canada Basin (leftmost diamonds). In this example, summer solar heating warms the surface such that the lateral density gradient is eliminated (red diamonds; the dotted line is $\sigma_0 = 22.3$ kg m^{-3}). (b) σ_0–τ plane with isolines of Θ (°C; blue lines) and S_A (g kg^{-1}; black lines). As temperature increases along an isopycnal (constant σ_0), the change in τ (kg m^{-3}) with respect to a change in temperature increases, while the tendency for spiciness is relatively insensitive to salinity.

functions in the Gibbs Seawater Oceanographic Toolbox that use the International Thermodynamic Equation of Seawater—2010 (TEOS-10; McDougall and Barker 2011; IOC et al. 2010). Along a constant density surface, the effects on density of changes in temperature $\delta\Theta$ and salinity δS_A are compensating (i.e., cancel each other) such that $\beta\delta S_A = \alpha\delta\Theta$. Therefore, the variation in water properties along isolines of density can be quantified as a measure that is proportional to $\beta\delta S_A$. The concept of a quantity related to temperature and salinity variations that do not affect the density was first introduced by Stommel (1962), more rigorously mathematically defined by Veronis (1972), and coined "spice" (for warm and salty) by Munk (1981). This is the principle of a spiciness variable and various forms have been derived (e.g., Veronis 1972; Jackett and McDougall 1985; Huang 2011; Flament 2002). Here, we use a spiciness variable τ, which is based on the requirement that its integral along an isoline of potential density σ (at a reference pressure $p_r = 0$ dbar) satisfies (McDougall and Krzysik 2015)

$$\int_\sigma d\tau = \int_\sigma \sigma(\alpha d\Theta + \beta dS_A) = 2\int_\sigma \sigma\beta\, dS_A,$$

where α and β are evaluated at $p_r = 0$. Spiciness τ, which has units of kilograms per cubic meter, is a differential quantity (its actual value depends upon the arbitrary choice of the constant of integration; McDougall and Krzysik 2015), and it is only appropriate to quote changes in τ along an isopycnal, not across isopycnals.

While the Arctic Ocean has a fascinating and complicated Θ–S_A structure, it is presently much less spicy than warmer oceans. At temperatures near freezing, increases in temperature have little effect on density because thermal kinetic expansion must compete with the weak hydrogen bonding that decreases the distance between water molecules. The coefficient of thermal expansion α is small at cold temperatures and increases with temperature such that it is about an order of magnitude larger at typical upper-ocean temperatures of the Pacific Ocean (~20°C) compared to the near-freezing Arctic Ocean. The strong temperature dependence of α (that gives rise to the curvature of σ contours on a temperature–salinity diagram; Fig. 1a) is a factor in the classification of α oceans (warmer oceans that are predominantly stratified by temperature) and β oceans, such as the Arctic Ocean, that are predominantly stratified by salinity (e.g., Carmack 2007). Near 0°C, the gradient in spice with respect to temperature is about 0.05 kg m^{-3} °C^{-1} for the range of densities of relevance in the oceans, while at about 20°C, it is an order of magnitude larger (Fig. 1b).

Stipa (2002) discusses the absence of spice in the context of the cold, brackish Baltic Sea (having salinities between 5 and 7 g kg^{-1}). Seawater has the property that for $S_A \lesssim 23.86$ g kg^{-1}, the temperature for which $\alpha = 0$°C^{-1} is warmer than the freezing temperature for a given salinity (Fig. 1a), and it is not possible for an increase in temperature to compensate an increase in salinity at temperatures near freezing. While the temperature of maximum density for a given salinity is the freezing

temperature for the much higher salinities of the Arctic Ocean, isopycnal salinity change tends to zero at these low temperatures; isolines of density and spiciness are nearly parallel (Fig. 2).

3. Water column structure: A Pacific–Arctic comparison

Water column profiles from the Arctic Ocean's central Canada Basin and from the western Pacific Ocean exemplify the stark differences in the structure of oceans that are predominantly stratified by salinity and warmer oceans that are predominantly stratified by temperature (Fig. 2). The nearly horizontal Arctic Ocean profile in the Θ–S_A plane shows the halocline stratification, characterized by cold temperatures and a strong increase in salinity with depth, while the nearly vertical Pacific Ocean profile in the Θ–S_A plane shows the thermocline stratification characterized by high salinities and a strong decrease in temperature with depth. Density differences due to salinity changes in the Arctic halocline are larger than density differences due to temperature changes by a factor of about 100. By contrast, in the Pacific thermocline, temperature changes dominate salinity changes in setting density by a factor of about 5.

a. Surface layer

Overlying the Pacific thermocline or the Arctic halocline, the vertically uniform density surface layer provides the dynamical link in the coupled atmosphere–ocean system. Arctic surface-layer dynamics mediate exchanges between warmer underlying waters and the overlying sea ice and atmosphere. In the midlatitude, ice-free oceans lateral variations in temperature and salinity in the surface layer are found to be density compensating on horizontal scales ranging from less than a kilometer to a hundred kilometers (Rudnick and Ferrari 1999; Ferrari and Rudnick 2000). While horizontal density gradients are minimal, horizontal gradients in temperature and salinity are not; the pervasive spiciness of the surface layer is a revealing signature of the ocean dynamics at play (Young 1994). Processes such as regionally variable atmospheric forcing set up lateral gradients in surface density. The resulting surface ocean fronts slump, and mixing destroys lateral density gradients, leaving behind only the observed density-compensated temperature–salinity gradients.

Beneath sea ice, however, the temperature–salinity relationship is of no use to infer dynamics since the Arctic Ocean surface layer in winter is almost always at the surface freezing temperature for seawater. That is, temperature collapses to a linear function of salinity, decreasing as salinity increases. While the Arctic Ocean surface layer displays a complicated structure with significant fronts and small eddies of a few kilometers (or less) in diameter, density compensation is not observed (Timmermans et al. 2012; Timmermans and Winsor 2013). Temperature by itself is, however, a useful passive tracer for understanding origins of the layered water masses in the Arctic halocline.

b. Thermocline/halocline intrusions

The interleaving of one water mass into another (giving rise to thermohaline intrusions, generally in the vicinity of frontal zones) is manifest by local extrema in temperature and salinity profiles. Intrusive features are best examined in the Θ–S_A plane where fingers extending along isopycnals show clearly how they provide an injection of spice (i.e., interleaving water masses of the same density are characterized by different temperature and salinity). The waters at the northern boundary of the Pacific Ocean's Kuroshio Extension, which transports warm water eastward from the coast of Japan (Jayne et al. 2009), often feature prominent intrusions (Okuda et al. 2001). The strong spiciness gradients indicate regions of intense lateral stirring of water masses and also contribute to enhanced diapycnal ocean mixing (Joyce 1977). The Pacific intrusions may be contrasted with warm intrusions in the Arctic halocline (Toole et al. 2010; Timmermans et al. 2014) measured in 2007 (Fig. 2), the second lowest sea ice extent in the 36-yr satellite record. While warm Arctic intrusions are characterized by marked deviations in temperature (implying strong lateral stirring), they are effectively spiceless (Fig. 2e). In a rare exception, arguably the warmest subsurface water observed in this sector of the Canada Basin in at least the past decade provides an example of spiciness in the Arctic and foretells a shift in the role of temperature under inevitable future warming (Fig. 3). In this extreme Arctic case, temperature is more than a passive tracer, and profiles show how the warm intrusion is characterized by anomalously high salinities, which are required to compensate its warm temperatures. For a 6°C temperature change along an isopycnal, the combined temperature–salinity compensation is around $1\,kg\,m^{-3}$, of comparable spiciness to the intrusive features in the Kuroshio Extension region (Fig. 2e). The presence of such warm intrusions in the Arctic halocline raises questions concerning their origins, their influence to sea ice cover and climate, and likely scenarios for the prevalence of such features in the future.

c. Ventilation of the thermocline/halocline

In the mid- to high-latitude ice-free oceans, seawater is transferred from the ocean surface into the thermocline by wind-driven subduction in regions where water masses with thermocline properties outcrop at the

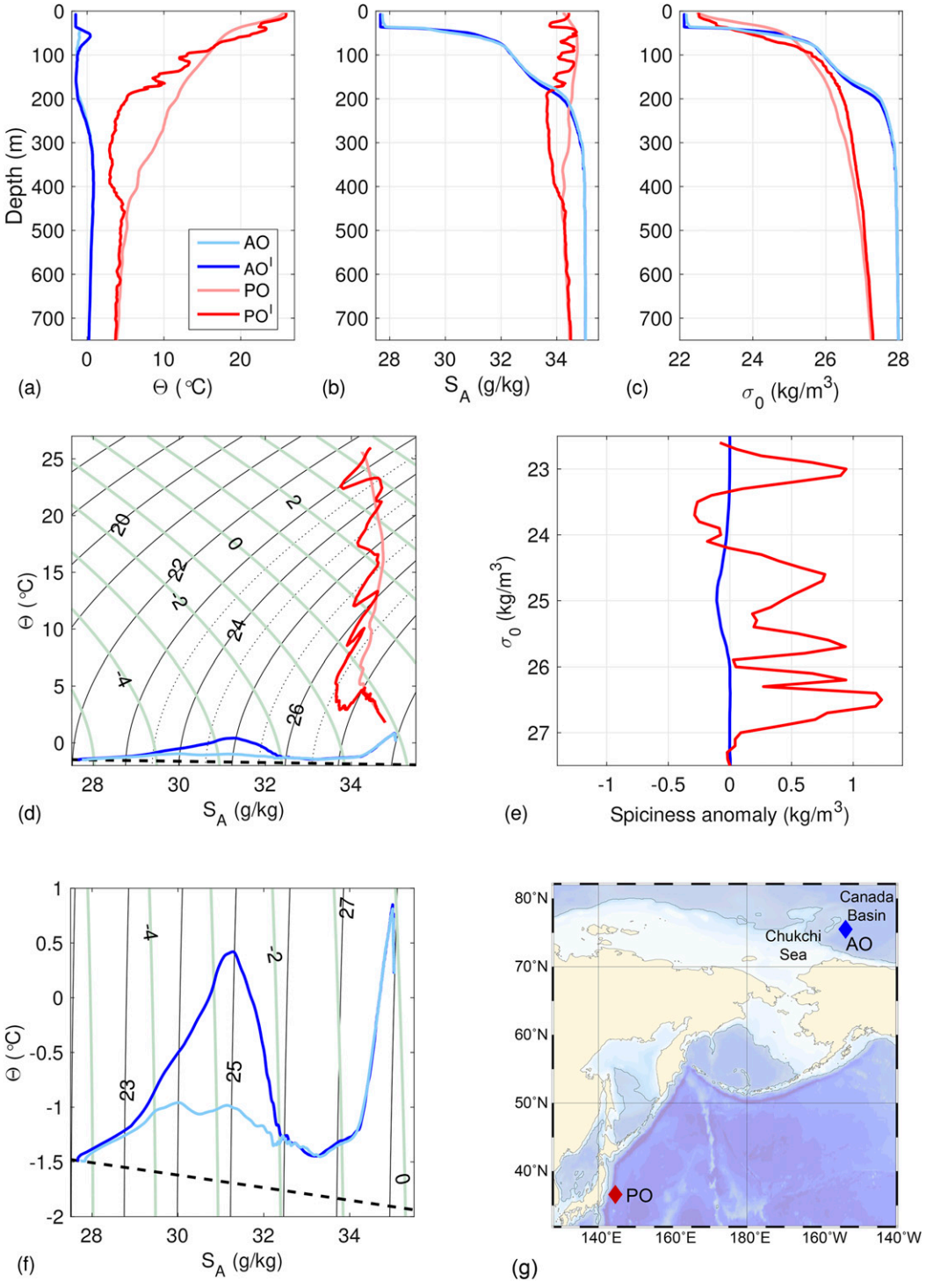

FIG. 2. (a) Conservative Temperature Θ (°C), (b) Absolute Salinity S_A (g kg^{-1}), and (c) potential density σ_0 (kg m^{-3}) profiles from the Arctic (~75°N, 155°W, separated by less than 10 km and less than 1 day in April 2007) and Pacific (~35°N, 145°E in the vicinity of the Kuroshio Extension frontal zone, separated by about 70 km and 10 days in September 2013) Oceans. Profiles with and without intrusions/interleaving are shown (the superscripts "I" on the legend labels indicate the profile with the intrusion); profiles are from a drifting Ice-Tethered Profiler (ITP 6) (Arctic) and Argo float (number 5904027; Pacific). (d) The same profiles in the Θ–S_A plane with isolines of potential density (black and dotted lines; kg m^{-3}) and spiciness (green lines; kg m^{-3}). The dashed black line indicates the freezing temperature at zero pressure. (e) The anomaly in spiciness on an isopycnal between each of the Arctic profiles (blue) and each of the Pacific profiles (red). (f) Close-up of the Arctic profiles in Θ–S_A space. (g) Map showing locations of Arctic Ocean (AO) and Pacific Ocean (PO) profiles.

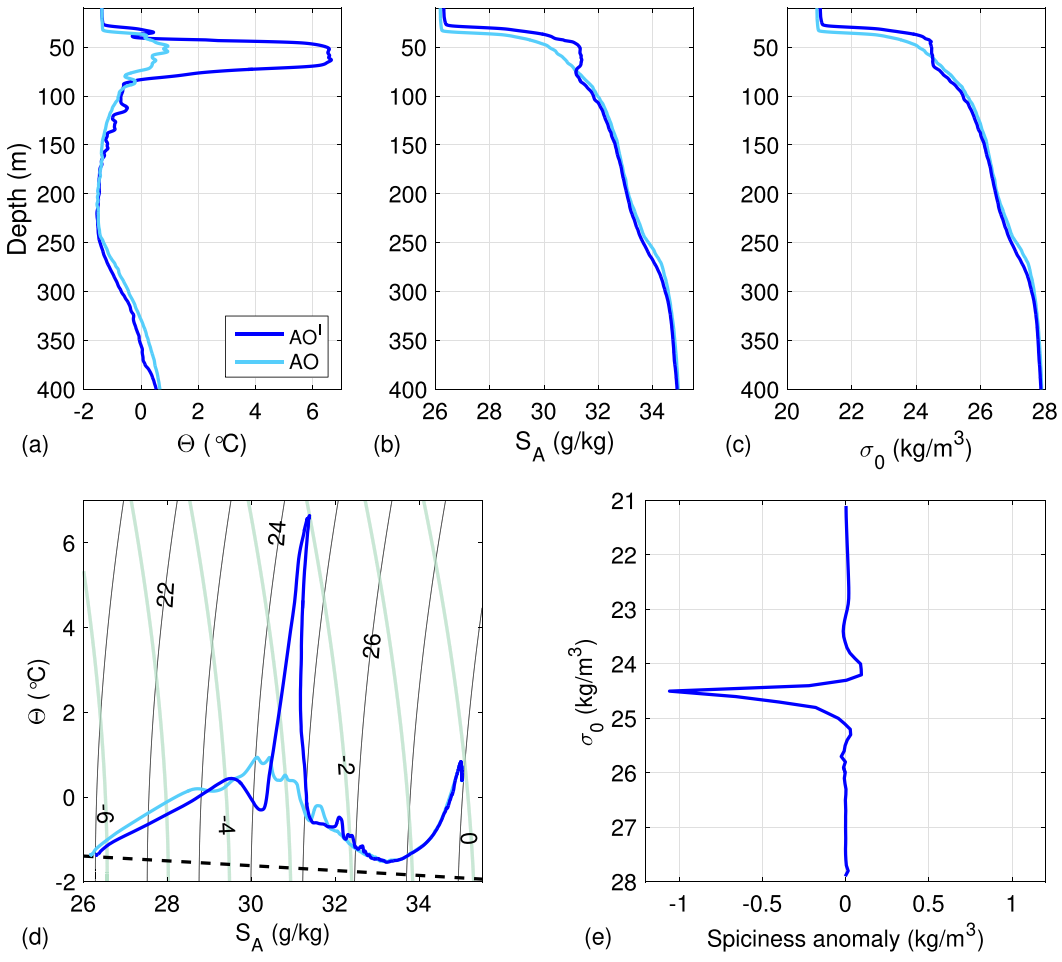

FIG. 3. As in Fig. 2, but an atypically spicy Arctic intrusion is shown (dark blue). Profiles are from an Ice-Tethered Profiler (ITP 33), and were taken less than 1 day and less than 10 km apart in November 2010, in the vicinity of the blue diamond shown in the inset map of Fig. 2.

surface (Iselin 1939; Stommel 1979). Stommel (1979) argued that fluid that subducts from the surface during the summer and fall (when mixed layers are shallowest and deepening) is entrained by the mixed layer deepening until the deepest mixed layers occur (in March), and only winter mixed layer fluid can be permanently subducted into the thermocline. This selection mechanism for fluid making up the main thermocline is referred to as "Stommel's demon" (Schmitt 1999). The correspondence between lateral surface gradients in density and spiciness, where temperature–salinity properties are set by surface atmospheric forcing and dynamical processes (Stommel 1993; Young 1994; Rudnick and Ferrari 1999), and vertical gradients in the subtropical gyre thermocline is an essential indicator of this process (Iselin 1939; Stommel 1979; Luyten et al. 1983).

Similar wind-driven dynamics apply to ventilation of the interior Arctic Ocean but with the potential to be fundamentally altered in a warming climate. In the Arctic Ocean's Canada Basin (Fig. 2g), the halocline is ventilated by the same mechanism as thermocline ventilation (Timmermans et al. 2014). Year-round, there exists a lateral surface salinity gradient from the Chukchi Sea to the fresher interior Canada Basin (the center of the wind-driven Beaufort Gyre; Proshutinsky et al. 2009). Wind stress curl pumping from an Ekman layer transfers fluid on isopycnals that outcrop at the surface in the Chukchi Sea down into the interior Canada Basin halocline; below the surface layer, water masses spread along isopycnals, while being advected to greater depths as they are swept along geostrophic contours in the Beaufort Gyre circulation. In this way, water warmed by solar insolation in ice-free regions in summer is archived at depth, away from the influence of surface atmospheric fluxes and wind-driven mixing.

Solar-warmed waters in the Chukchi Sea give rise to warm interleaving layers in the halocline, with the atypically warm intrusions observed in the Canada Basin

in recent years deriving from intense summertime solar warming on outcropping isopycnals in expansive ice-free regions (Timmermans et al. 2014). Associated with the substantially reduced sea ice cover in 2007, for example, sea surface temperatures were anomalously warm in the Chukchi Sea; that same year saw halocline ventilation by warm intrusions in the Canada Basin (Fig. 2). This is a conduit for solar-warmed water to be transported to the halocline, where it has the potential to melt or slow the growth of sea ice in the fall and winter (e.g., Timmermans 2015). Except in rare cases (Fig. 3), the summer solar warming is not sufficient for temperature to influence the density of warm intrusions.

Under future warming and reduced sea ice cover, however, solar absorption into the surface ocean may be sufficiently intense that the lateral density gradient between warm, salty water in the Chukchi Sea and cool, freshwater at the surface in the Canada Basin is reduced or eliminated (Fig. 1a). In this case, as solar warming commences in summer, the surface water in the Chukchi Sea becomes closer in density to the surface Canada Basin water. Because of the nonlinear equation of state, only a small lateral gradient in surface heating is required to eliminate the surface density gradient because density changes in response to heating are much smaller for the cooler water (Fig. 1a). Reduced lateral stratification results from preferential warming of the saltiest surface water in the Chukchi Sea (solar absorption is inhibited where sea ice persists for longer in the Canada Basin). This leads to warmed waters being pumped to shallower depths in the halocline (assuming, in this scenario, no change in the wind stress curl field). An example is provided by the anomalously spicy Arctic intrusion (Fig. 3), which was sufficiently warm that it ventilated the water column about 30 m closer to the surface than if temperature had not had any effect on density. If warming is sufficient to eliminate the lateral surface density gradient (the example shown in Fig. 1a), halocline ventilation by surface waters will be shut off because deep isopycnals will no longer outcrop at the surface. In the example, this happens once the relatively warm and salty surface of the Chukchi Sea is warmed by about 7°C (to 13°C), the rightmost diamonds in Fig. 1a. This temperature increase corresponds to about 200 $W m^{-2}$ incoming solar radiation (cf. Perovich et al. 2007) to the surface ocean (in the absence of sea ice cover and assuming the net summer heat input is dominated by the absorption of solar radiation) over a period of about 1.5 months for typical mixed layer thicknesses of a few tens of meters—a magnitude of warming that is inevitable given the anticipated longer durations of open water in the future. This illustrates that if seasonal warming is sufficient to appreciably modify the density of the surface layer, there is a limit to the heat that may be stored in the halocline. Summer warming in excess of this limit will be lost rapidly to the atmosphere upon fall cooling, rather than being stored at depth.

Future warming and reduced Arctic sea ice will impose a seasonal selection mechanism on ventilating waters. This is the extent of the analogy with Stommel's demon that describes the exclusion from the permanent thermocline of waters that leave the mixed layer in the summer/fall in the North Atlantic. In the Arctic, the halocline will remain unventilated during times when the mixed layer is warmest and deep isopycnals no longer outcrop into the mixed layer, analogous to the unventilated shadow zones in the eastern subtropical gyre regions of the midlatitudes.

d. Double diffusion

In his article "Spice and the Demon," Schmitt (1999) suggested that the differential mixing of heat and salt by double-diffusive convection sets the well-defined relationship between temperature and salinity in ocean thermoclines, supplying an explanation for observations to be consistent with the theory of the ventilated thermocline (Schmitt 1981). The Arctic Ocean is well known for its laterally coherent, interleaving, double-diffusive intrusions (Carmack et al. 1998; Woodgate et al. 2007) and double-diffusive staircases (Padman and Dillon 1987; Timmermans et al. 2008), but these double-diffusive processes are deeper than the ventilated halocline in the Canada Basin. Although the concept of variations in temperature and salinity along isopycnals is useful in the identification of double-diffusive intrusions (e.g., May and Kelley 2001), these features are at least an order of magnitude less spicy than the shallower Pacific halocline intrusions (e.g., Figs. 2, 3). While Arctic double-diffusive structures show an impressive persistence and finestructure, double-diffusive heat fluxes remain weak. Double-diffusive heat fluxes compose only a small fraction of ocean-to-ice heat fluxes in the salinity-stratified waters (Timmermans et al. 2008), and the impacts of a changing climate on these waters remain to be seen.

4. Summary

In the present Arctic, temperature has a negligible effect on density, and summertime solar-warmed water has a pathway to ventilate the halocline. Under continued warming, ocean temperature will play an increasingly dynamic role in the Arctic Ocean. Interleaving layers that are warmer and spicier will be a common occurrence in the halocline. The classic halocline characterized by monotonically increasing salinity with depth will be displaced by a more complex pycnocline in

which interleaving layers are sufficiently warm that they must be compensated by reversals in the salinity gradient. When warming is sufficient to eliminate the lateral density gradient of the surface waters, the wind-driven ventilation pathway for summertime solar-warmed water into the halocline will be shut off entirely during the warmest periods. In a warmer, spicier Arctic Ocean, the transport of ocean heat, and the capacity for its archival at depth, will be no longer entirely dependent on vertical and lateral salinity gradients. These new dynamics will contribute to ongoing changes impacting the links among the Arctic Ocean, sea ice, and climate.

Acknowledgments. The Ice-Tethered Profiler data were collected and made available by the Ice-Tethered Profiler Program based at the Woods Hole Oceanographic Institution (Krishfield et al. 2008; Toole et al. 2011; http://www.whoi.edu/itp). Argo profiling float data were collected and made available by the International Argo Program, part of the Global Ocean Observing System (http://www.argo.ucsd.edu; http://argo.jcommops.org; doi:10.12770/934715ad-8c42-4382-86c5-e0dbdf868b53). Support was provided by the National Science Foundation Division of Polar Programs Award 1350046 and Office of Naval Research Grant Number N00014-12-1-0110.

REFERENCES

Aagaard, K., and P. Greisman, 1975: Toward new mass and heat budgets for the Arctic Ocean. *J. Geophys. Res.*, **80**, 3821–3827, doi:10.1029/JC080i027p03821.

Carmack, E. C., 2007: The alpha/beta ocean distinction: A perspective on freshwater fluxes, convection, nutrients and productivity in high-latitude seas. *Deep-Sea Res. II*, **54**, 2578–2598, doi:10.1016/j.dsr2.2007.08.018.

——, K. Aagaard, J. H. Swift, R. G. Perkin, F. A. McLaughlin, R. W. Macdonald, and E. P. Jones, 1998: Thermohaline transitions. Physical Processes in Lakes and Oceans, Coastal and Estuarine Studies Series, Vol. 54, Amer. Geophys. Union, 179–186.

Ferrari, R., and D. L. Rudnick, 2000: Thermohaline variability in the upper ocean. *J. Geophys. Res.*, **105**, 16 857–16 883, doi:10.1029/2000JC900057.

Flament, P., 2002: A state variable for characterizing water masses and the diffusive stability: Spiciness. *Prog. Oceanogr.*, **54**, 493–501, doi:10.1016/S0079-6611(02)00065-4.

Francis, J. A., W. Chan, D. J. Leathers, J. R. Miller, and D. E. Veron, 2009: Winter Northern Hemisphere weather patterns remember summer Arctic sea-ice extent. *Geophys. Res. Lett.*, **36**, L07503, doi:10.1029/2009GL037274.

Huang, R. X., 2011: Defining the spicity. *J. Mar. Res.*, **69**, 545–559, doi:10.1357/002224011799849390.

IOC, SCOR, and IAPSO, 2010: The International Thermodynamic Equation of Seawater—2010: Calculation and use of thermodynamic properties. Intergovernmental Oceanographic Commission, Manuals and Guides 56, 220 pp. [Available online at http://www.teos-10.org/pubs/TEOS-10_Manual.pdf.]

Iselin, C., 1939: The influence of vertical and lateral turbulence on the characteristics of the waters at mid-depths. *Eos, Trans. Amer. Geophys. Union*, **20**, 414–417, doi:10.1029/TR020i003p00414.

Jackett, D. R., and T. J. McDougall, 1985: An oceanographic variable for the characterization of intrusions and water masses. *Deep-Sea Res. I*, **32**, 1195–1207, doi:10.1016/0198-0149(85)90003-2.

Jayne, S. R., and Coauthors, 2009: The Kuroshio Extension and its recirculation gyres. *Deep-Sea Res. I*, **56**, 2088–2099, doi:10.1016/j.dsr.2009.08.006.

Joyce, T. M., 1977: A note on the lateral mixing of water masses. *J. Phys. Oceanogr.*, **7**, 626–629, doi:10.1175/1520-0485(1977)007<0626:ANOTLM>2.0.CO;2.

Krishfield, R., J. Toole, A. Proshutinsky, and M.-L. Timmermans, 2008: Automated ice-tethered profilers for seawater observations under pack ice in all seasons. *J. Atmos. Oceanic Technol.*, **25**, 2091–2105, doi:10.1175/2008JTECHO587.1.

Luyten, J., J. Pedlosky, and H. Stommel, 1983: The ventilated thermocline. *J. Phys. Oceanogr.*, **13**, 292–309, doi:10.1175/1520-0485(1983)013<0292:TVT>2.0.CO;2.

May, B. D., and D. E. Kelley, 2001: Growth and steady state stages of thermohaline intrusions in the Arctic Ocean. *J. Geophys. Res.*, **106**, 16 783–16 794, doi:10.1029/2000JC000605.

Maykut, G. A., and N. Untersteiner, 1971: Some results from a time-dependent thermodynamic model of sea ice. *J. Geophys. Res.*, **76**, 1550–1575, doi:10.1029/JC076i006p01550.

McDougall, T. J., and P. M. Barker, 2011: Getting started with TEOS-10 and the Gibbs Seawater (GSW) oceanographic toolbox. SCOR/IAPSO WG127, 28 pp. [Available online at www.teos-10.org/pubs/Getting_Started.pdf.]

——, and O. A. Krzysik, 2015: Spiciness. *J. Mar. Res.*, **73**, 141–152, doi:10.1357/002224015816665589.

Munk, W., 1981: Internal waves and small-scale processes. *Evolution of Physical Oceanography*, B. A. Warren and C. Wunsch, Eds., MIT Press, 264–291.

Okuda, K., I. Yasuda, Y. Hiroe, and Y. Shimizu, 2001: Structure of subsurface intrusion of the Oyashio water into the Kuroshio Extension and formation process of the North Pacific Intermediate Water. *J. Phys. Oceanogr.*, **57**, 121–140, doi:10.1023/A:1011135006278.

Padman, L., and T. M. Dillon, 1987: Vertical heat fluxes through the Beaufort Sea thermohaline staircase. *J. Geophys. Res.*, **92**, 10 799–10 806, doi:10.1029/JC092iC10p10799.

Perovich, D. K., S. V. Nghiem, T. Markus, and A. Schweiger, 2007: Seasonal evolution and interannual variability of the local solar energy absorbed by the Arctic sea ice–ocean system. *J. Geophys. Res.*, **112**, C03005, doi:10.1029/2006JC003558.

——, J. A. Richter-Menge, K. F. Jones, and B. Light, 2008: Sunlight, water, and ice: Extreme Arctic sea ice melt during the summer of 2007. *Geophys. Res. Lett.*, **35**, L11501, doi:10.1029/2008GL034007.

Proshutinsky, A., and Coauthors, 2009: Beaufort Gyre freshwater reservoir: State and variability from observations. *J. Geophys. Res.*, **114**, C00A10, doi:10.1029/2008JC005104.

Rudnick, D. L., and R. Ferrari, 1999: Compensation of horizontal temperature and salinity gradients in the ocean mixed layer. *Science*, **283**, 526–529, doi:10.1126/science.283.5401.526.

Schmitt, R. W., 1981: Form of the temperature-salinity relationship in the Central Water: Evidence for double-diffusive

mixing. *J. Phys. Oceanogr.*, **11**, 1015–1026, doi:10.1175/1520-0485(1981)011<1015:FOTTSR>2.0.CO;2.

——, 1999: Spice and the demon. *Science*, **283**, 498–499, doi:10.1126/science.283.5401.498.

Steele, M., W. Ermold, and J. Zhang, 2008: Arctic Ocean surface warming trends over the past 100 years. *Geophys. Res. Lett.*, **35**, L02614, doi:10.1029/2007GL031651.

Stipa, T., 2002: Temperature as a passive isopycnal tracer in salty, spiceless oceans. *Geophys. Res. Lett.*, **29**, 1953, doi:10.1029/2001GL014532.

Stommel, H. M., 1962: On the cause of the temperature-salinity curve in the ocean. *Proc. Natl. Acad. Sci. USA*, **48**, 764–766, doi:10.1073/pnas.48.5.764.

——, 1979: Determination of water mass properties of water pumped down from the Ekman layer to the geostrophic flow below. *Proc. Natl. Acad. Sci. USA*, **76**, 3051–3055, doi:10.1073/pnas.76.7.3051.

——, 1993: A conjectural regulating mechanism for determining the thermohaline structure of the oceanic mixed layer. *J. Phys. Oceanogr.*, **23**, 142–148, doi:10.1175/1520-0485(1993)023<0142:ACRMFD>2.0.CO;2.

Timmermans, M.-L., 2015: The impact of stored solar heat on Arctic sea ice growth. *Geophys. Res. Lett.*, **42**, 6399–6406, doi:10.1002/2015GL064541.

——, and P. Winsor, 2013: Scales of horizontal density structure in the Chukchi Sea surface layer. *Cont. Shelf Res.*, **52**, 39–45, doi:10.1016/j.csr.2012.10.015.

——, J. Toole, R. Krishfield, and P. Winsor, 2008: Ice-tethered profiler observations of the double-diffusive staircase in the Canada basin thermocline. *J. Geophys. Res.*, **113**, C00A02, doi:10.1029/2008JC004829.

——, S. Cole, and J. Toole, 2012: Horizontal density structure and restratification of the Arctic Ocean surface layer. *J. Phys. Oceanogr.*, **42**, 659–668, doi:10.1175/JPO-D-11-0125.1.

——, and Coauthors, 2014: Mechanisms of Pacific Summer Water variability in the Arctic's central Canada basin. *J. Geophys. Res. Oceans*, **119**, 7523–7548, doi:10.1002/2014JC010273.

Toole, J. M., M.-L. Timmermans, D. K. Perovich, R. A. Krishfield, A. Proshutinsky, and J. Richter-Menge, 2010: Influences of the ocean surface mixed layer and thermohaline stratification on Arctic sea ice in the central Canada basin. *J. Geophys. Res.*, **115**, C10018, doi:10.1029/2009JC005660.

——, R. A. Krishfield, M.-L. Timmermans, and A. Proshutinsky, 2011: The ice-tethered profiler: Argo of the Arctic. *Oceanography*, **24**, 126–135, doi:10.5670/oceanog.2011.64.

Veronis, G., 1972: On the properties of seawater defined by temperature, salinity and pressure. *J. Mar. Res.*, **30**, 227–255.

Wettlaufer, J., 1991: Heat flux at the ice-ocean interface. *J. Geophys. Res.*, **96**, 7215–7236, doi:10.1029/90JC00081.

Woodgate, R. A., K. Aagaard, J. H. Swift, W. M. Smethie, and K. K. Falkner, 2007: Atlantic water circulation over the Mendeleev Ridge and Chukchi Borderland from thermohaline intrusions and water mass properties. *J. Geophys. Res.*, **112**, C02005, doi:10.1029/2005JC003416.

Young, W., 1994: The subinertial mixed layer approximation. *J. Phys. Oceanogr.*, **24**, 1812–1826, doi:10.1175/1520-0485(1994)024<1812:TSMLA>2.0.CO;2.